Supplementary Information

Oxidative degradation of cylindrospermopsin and anatoxin-a by Fe^{III}-B*/H_2O_2

Jishan Liu[a], *David R. Greenwood*[b], *Lionel Kuntz*[c], *L. James Wright*[c,]*, *Naresh Singhal*[a,]*

[a] Department of Civil & Environmental Engineering, University of Auckland, Auckland 1142, New Zealand

[b] School of Biological Sciences, University of Auckland, Auckland 1142, New Zealand

[c] School of Chemical Sciences, University of Auckland, Auckland 1142, New Zealand

* Corresponding Authors: Associate Professor Naresh Singhal and Professor L. James Wright

Email: n.singhal@auckland.ac.nz; lj.wright@auckland.ac.nz

Tel: + 64 9 923 4512, +64 9 923 8257

1. Influence of pH on oxidative removal of cyanotoxin by Fe^{III}-B*/H_2O_2

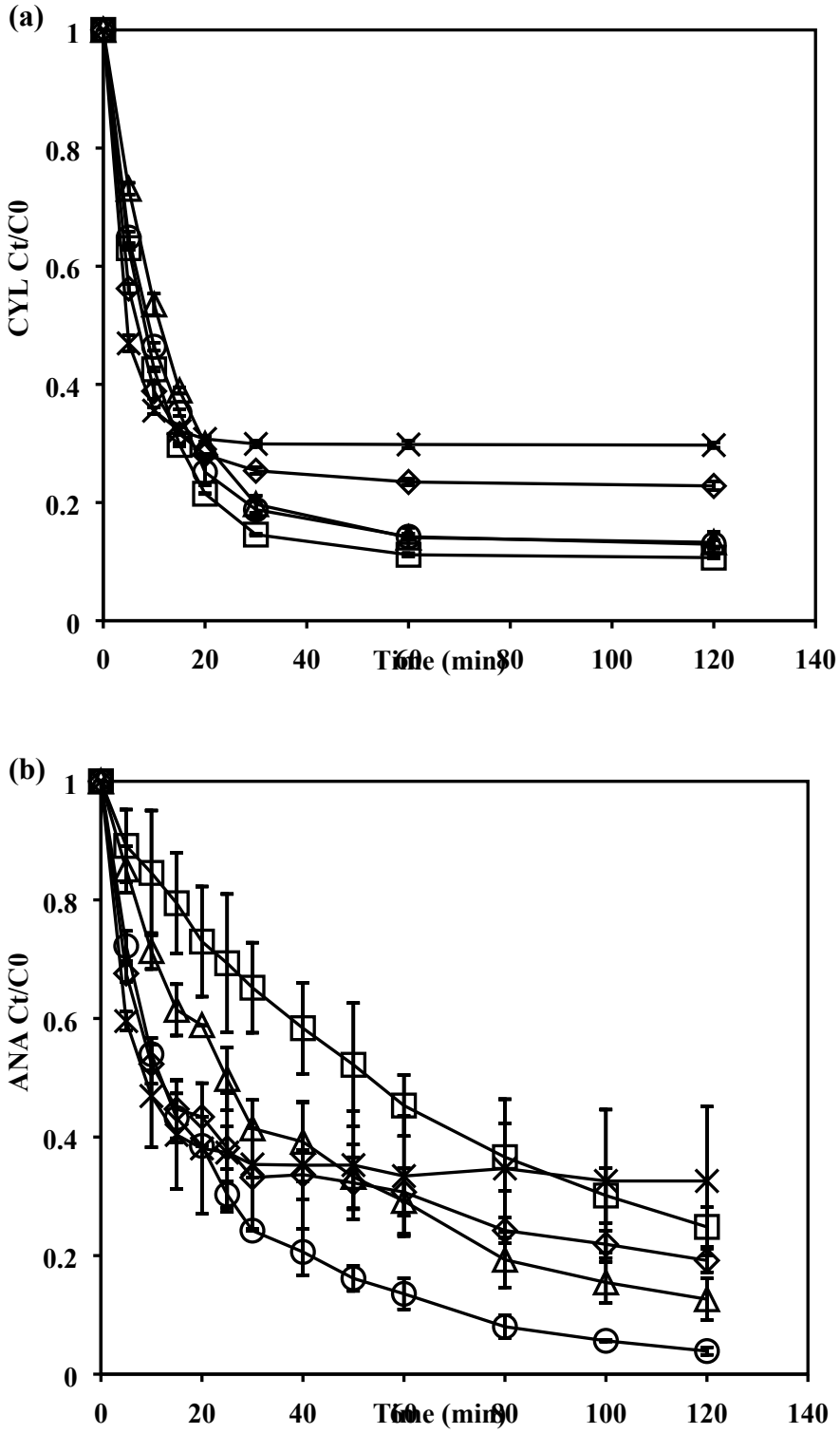

Figure S1: Removal of cyanotoxins by Fe^{III}-B*/H_2O_2 at different pH values. (a) CYL (0.24 µM) and (b) ANA (7.1 µM) removal by Fe^{III}-B*/H_2O_2 (5.0 µM/ 5.0 mM) at pH 8.5 (□), 9.0 (Δ), 9.5 (○), 10.5 (◊) and 11.5 (x) (0.01 M) (mean ± standard deviation of three independent runs).

2. Immobilizing Fe^{III}-B* catalyst onto the functionalised silica gel

To generate the immobilized Fe^{III}-B* catalyst, the silica gel was firstly functionalized (1-3), and then Fe^{III}-B* catalyst was adsorbed from aqueous solution (4-6). In Step 1, 5 g silica gel was treated with 7 mL DMOAP solution in 63 mL water for 2 hrs at 60 °C with stirring (300 rpm). The functionalized silica gel, Si-DMOAP, was recovered by filtration and washed thoroughly with water (3×50 mL) and acetone (3×50 mL) and then dried in a vacuum oven at 110 °C overnight. In Step 2, 2.5×10^{-7} mole, 1.25×10^{-6} mole or 2.5×10^{-6} moles Fe^{III}-B* in pH 9.5 buffer solution (50 mL, 0.01 M $Na_2CO_3/NaHCO_3$) was stirred with Si-DMOAP (240 mg) at 300 rpm. Fe^{III}-B*/Si-DMOAP was collected by filtration after 15 min.

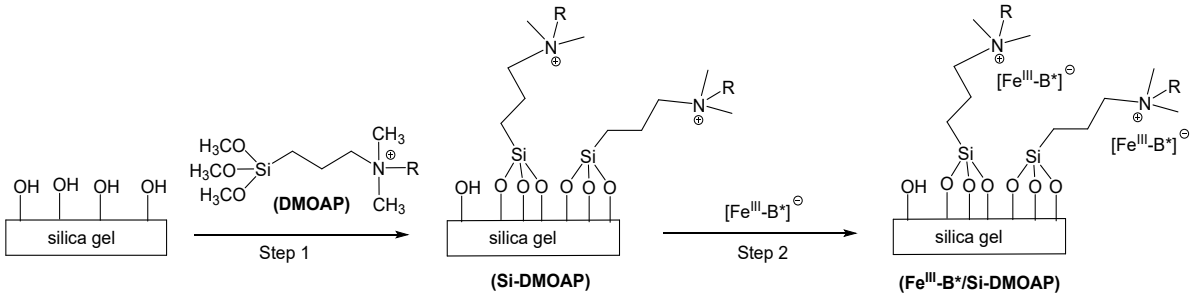

Scheme S1: Covalent attachment of quaternary ammonium reagent to silica gel and immobilisation of Fe^{III}-B* catalyst onto the functionalised silica gel.

3. Coverage assessment of Fe^{III}-B*/Si-DMOAP

The amount of Fe^{III}-B* adsorbed onto Si-DMOAP was quantified by determining the residual Fe^{III}-B* remaining in the filtrate and the Fe^{III}-B* released during washing of Fe^{III}-B*/Si-DMOAP with buffer solution. The residual Fe^{III}-B* in each solution was determined by monitoring the rate of bleaching of orange II under standard conditions. To wash Fe^{III}-B*/Si-DMOAP, it was re-suspension in buffer solution (50 mL) for 15 minutes and then filtered and the concentration of leached Fe^{III}-B* determined. This process was repeated until the amount of Fe^{III}-B* released each time was constant. The total released Fe^{III}-B* was calculated by summing the amount of Fe^{III}-B* not initially adsorbed and that released into each of the buffer solutions (Scheme S2). To determine the Fe^{III}-B* concentration of each solution, orange II was

added to give a final concentration of 45 μM and pH 9.5 0.01 M $Na_2CO_3/NaHCO_3$ buffer used to make the solution up to 100 mL. Dye bleaching was initiated by adding H_2O_2 (e.g., 0.102 mL of 0.979 mol L^{-1} solution) to each solution to give a final concentration of 1.00 mM and the absorbance at 464.5 nm recorded at set intervals. The amount of Fe^{III}-B* in the filtrates was determined by measuring the initial rate of bleaching and then using a calibration curve to determine the Fe^{III}-B* concentration.

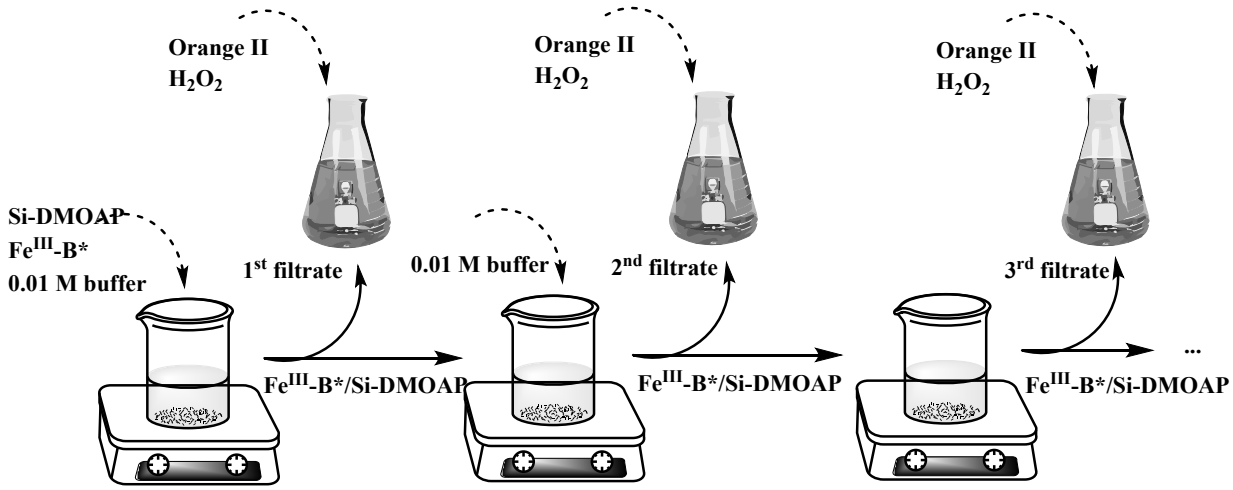

Scheme S2: The process flow diagram for the immobilized Fe^{III}-B* coverage testing.

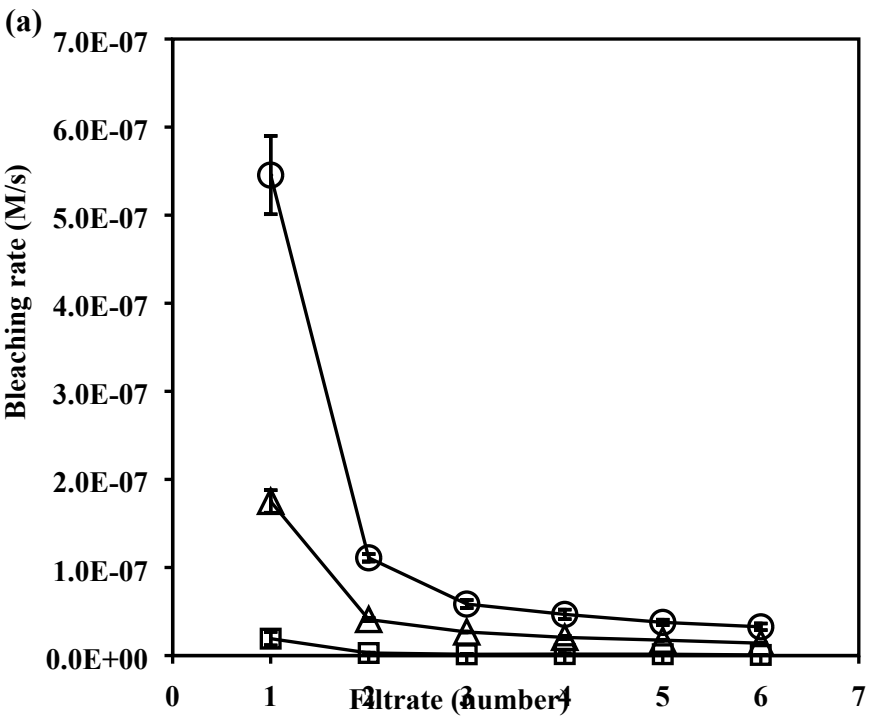
(a)
7.0E-07
6.0E-07
5.0E-07
4.0E-07
3.0E-07
2.0E-07
1.0E-07
0.0E+00
Bleaching rate (M/s)
0
1
2
3
4
5
6
7
Filtrate (number)

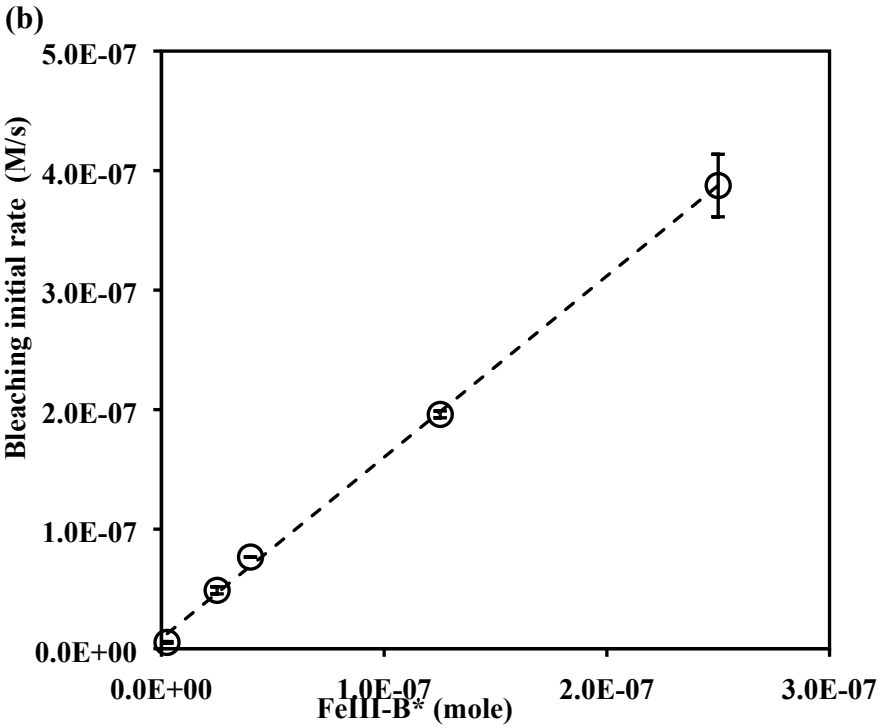
(b)
5.0E-07
4.0E-07
3.0E-07
2.0E-07
1.0E-07
0.0E+00
Bleaching initial rate (M/s)
0.0E+00
1.0E-07
2.0E-07
3.0E-07
FeIII-B* (mole)

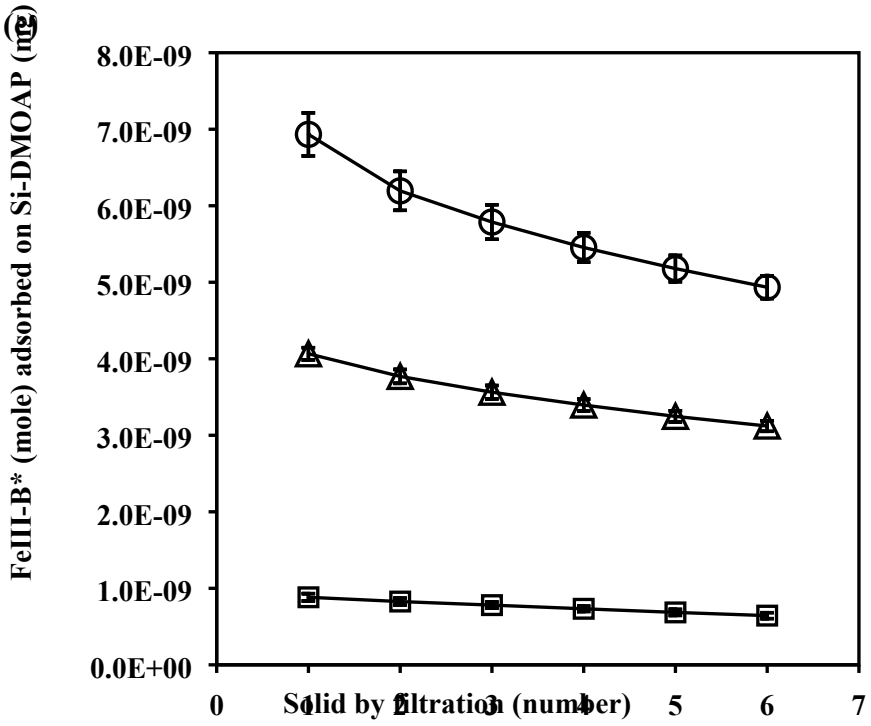

Figure S2: Assessment of the amount of Fe^{III}-B* adsorbed on Si-DMOAP. (a) The initial rates of orange II dye (45 μM) bleaching catalysed by residual Fe^{III}-B* in the filtrate from immobilized Fe^{III}-B* catalyst generation, by different amount of initial Fe^{III}-B* (2.5×10^{-6} (○), 1.25×10^{-6} (Δ) and 2.5×10^{-7} (□) mole dissolved Fe^{III}-B* and 240 mg Si-DMOAP) and H_2O_2 (1 mM) at pH 9.5 (0.01 M); (b) a calibraiton curve of the initial rates of orange II dye (45 μM) bleaching by Fe^{III}-B* standards (2.5×10^{-9}, 2.5×10^{-8}, 4×10^{-8}, 1.25×10^{-7} and 2.5×10^{-7} mole) and H_2O_2 (1.0 mM) in 100 mL pH 9.5 0.01 M Na_2CO_3/$NaHCO_3$ buffer solution; (c) the amount of Fe^{III}-B* (mole) adsorbed onto functionalised silica gel (mg) (mean ± standard deviation of three independent runs).

Based on the assessment of the amount of Fe^{III}-B* (2.5×10^{-7} mole) adsorbed onto Si-DMOAP, the coverage ratio that was measured for the fourth filtration indicated a constant amount of Fe^{III}-B* was released. This was confirmed by comparing to the results for the fifth and sixth filtration. Consequently, Fe^{III}-B*/Si-DMOAP collected from the fourth filtration was applied to the treatment of cyanotoxins.

4. Solid-phase extraction procedure

The CYL-SPE method was modified from Metcalf, Beattie (7) and Foss and Aubel (8) with the application of Hypersep Hypercarb SPE cartridges (Thermo Fisher Scientific, NZ Ltd.): 1) cartridges were conditioned with two column volumes of methanol and rinsed with two column

volumes of water; 2) samples were loaded onto cartridges at a flow rate of 1 − 2 mL/min; 3) cartridges were washed with one column volume of water and fully air-dried prior to elution; and 4) CYL was eluted with 5 % formic acid in methanol (3×500 μL). The ANA-SPE using Strata-X-CW polymeric weak cation SPE cartridges (Phenomenex Australia Ply Ltd.) was conducted as follows: (1) one column volume of methanol followed by one column volume of water was applied to condition the cartridges; (2) samples were loaded after adjustment to pH 6 ~ 7; (3) one column volume of water followed by one column volume of methanol was used to wash the cartridges; and (4) samples were eluted with 5 % formic acid in methanol (3×500 μL). For all SPE samples, the eluate was evaporated to dryness in a speed vacuum concentrator (Savant SPD131DDA, ThermoFisher) and then reconstituted in methanol (1 mL) for analysis.

5. Cyanotoxin removal by Fe^{III}-B*/H_2O_2 with NOM or with oxidized NOM at pH 9.5 (0.01 M)

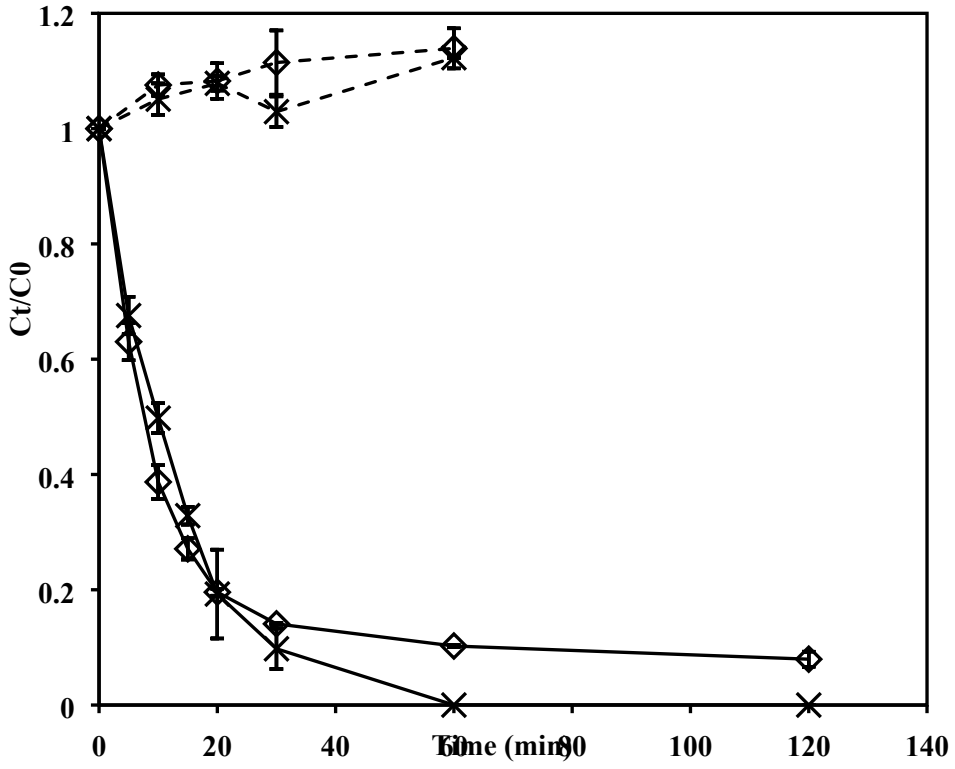

Figure S3: Cyanotoxin removal by Fe^{III}-B*/H_2O_2 with NOM or with oxidized NOM at pH 9.5 (0.01 M). ─◊─ represents sample of CYL (0.24 µM) with NOM (3.5 ppm) removal by Fe^{III}-B*/H_2O_2 (5 µM/ 5 mM), ─x─ represents sample of ANA (7.1 µM) with NOM (30 ppm) removal by Fe^{III}-B*/H_2O_2 (5 µM/ 5 mM), - -◊- - represents sample of CYL (0.24 µM) removal by oxidized NOM (3.5 ppm), - -x- - represents sample of ANA (7.1 µM) removal by oxidized NOM (30 ppm) (mean ± standard deviation of three independent runs).

Oxidized NOM was produced by NOM (3.5 ppm NOM designated for CYL; 30 ppm NOM designated for ANA) reacting with Fe^{III}-B*/H_2O_2 (5 µM/ 5 mM) at pH 9.5 0.01 M Na_2CO_3/$NaHCO_3$ buffer. Reacting NOM was taken at intervals and treated with catalase. The oxidized NOM was then mixed with CYL (0.24 µM) or ANA (7.1 µM) thoroughly. Cyanotoxin was quantified by LC-MS.

6. Fluorophore signatures of NOM oxidized by Fe^{III}-B*/H_2O_2

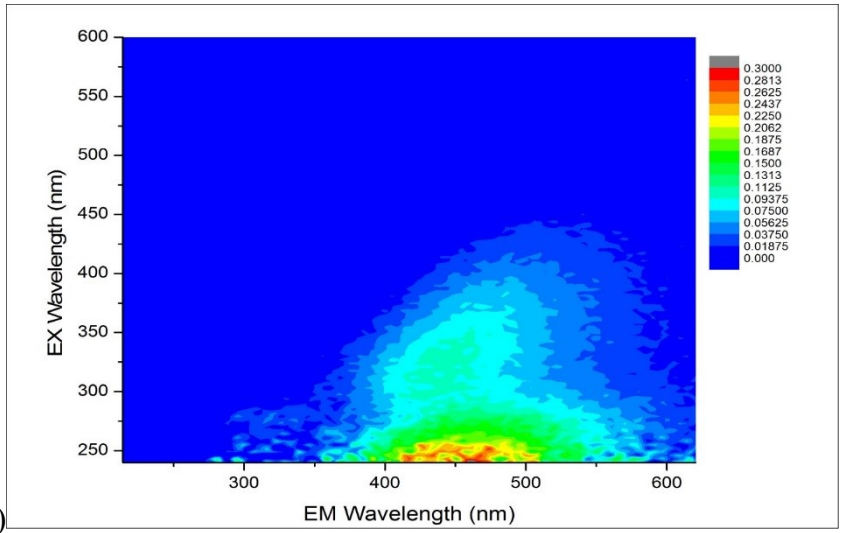

(a)

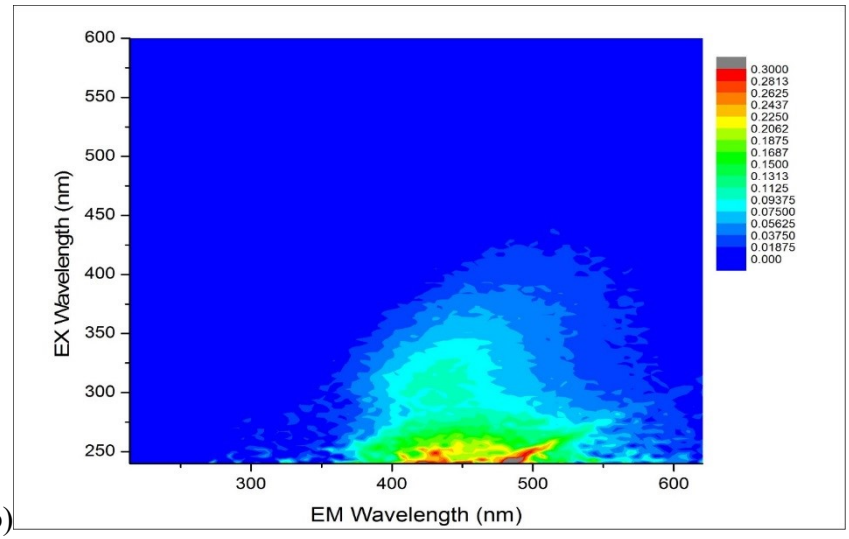

(b)

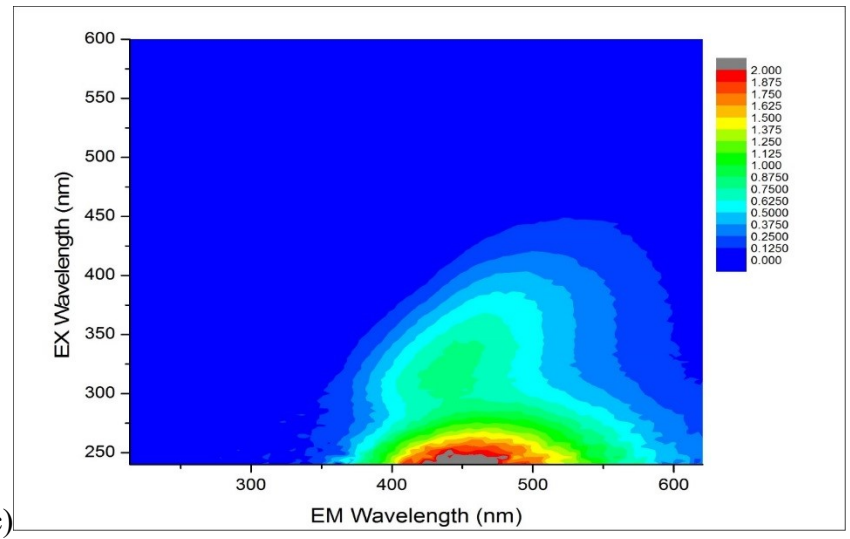

(c)

(d) 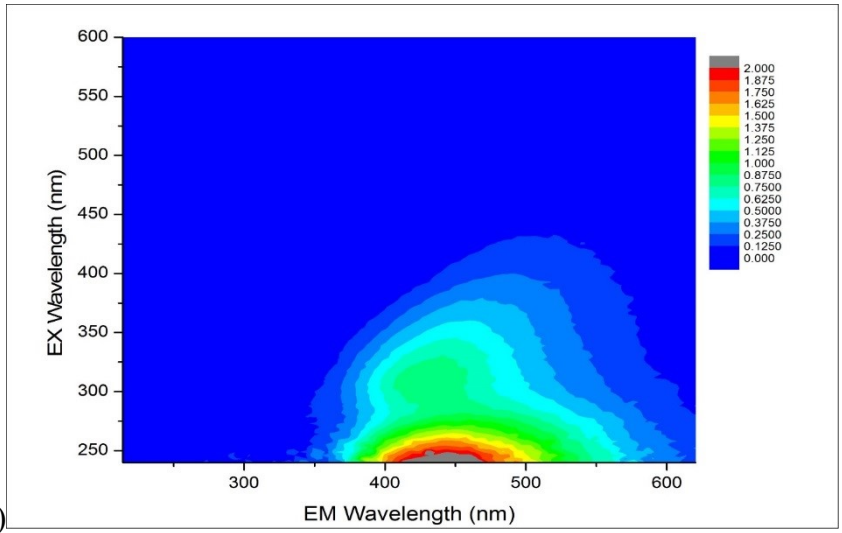

Figure S4: Fluorophore signatures of NOM oxidized by Fe^{III}-B*/H_2O_2. (a) NOM (3.5 ppm) with Fe^{III}-B* (5 µM) at pH 9.5 (0.01 M); (b) NOM (3.5 ppm) oxidized by Fe^{III}-B*/H_2O_2 (5 µM/ 5 mM) at pH 9.5 (0.01 M); (c) NOM (30 ppm) with Fe^{III}-B* (5 µM) at pH 9.5 (0.01 M); (d) NOM (30 ppm) oxidized by Fe^{III}-B*/H_2O_2 (5 µM/ 5 mM) at pH 9.5 (0.01 M). Ex 270 − 280/Em 310 − 320 for tyrosine-like and protein-like materials, Ex 270 − 285/Em 340 − 360 for tryptophan-like and protein-like matter, Ex 320 − 350/Em 400 − 450 for fulvic-like matter, Ex 310 − 320/Em 380 − 420 and Ex 330 − 390/Em 420 − 500 for humic-like matter (9).

7. Positive mode Q-Exactive tandem mass spectra of CYL

(a)

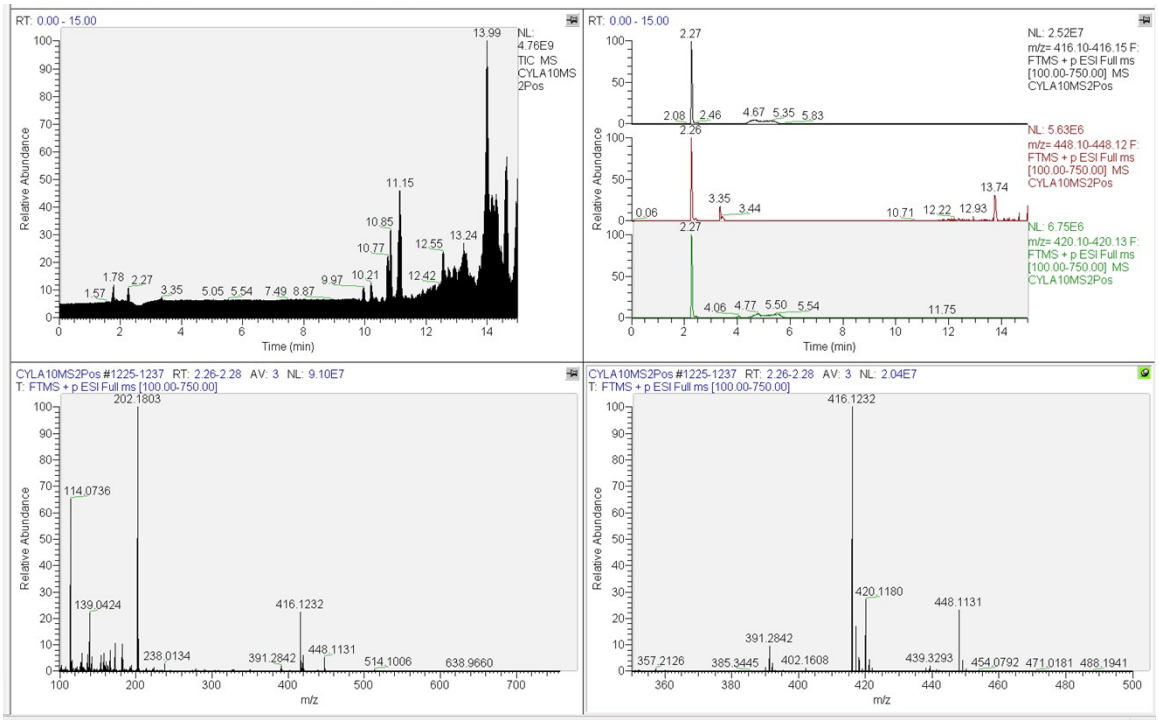

(b)

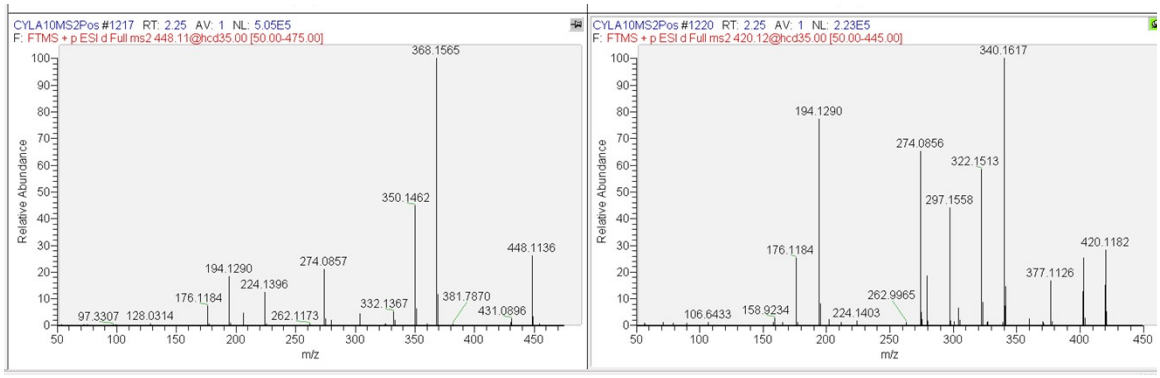

Figure S5: (a) Reaction product ion spectrum MS^1 for ions eluting at 2.27 min and reconstructed ion chromatograms showing elution profiles of three ions (*m/z* 416, 448 and 420); (b) CID product ion spectra MS^2 for ion *m/z* 448 eluting at 2.25 min, and *m/z* 420 eluting at 2.25 min.

With reference to the software Mass FrontierTM and Xcalibur, the MS2 fragment m/z 350.1462 (1b, 1b', or 1b'') could be generated via a number of transformation routes including hydrogen abstraction at C8 and hydrogen sulfate removal from the product with m/z 448.1131 (1) and, water elimination from the product with m/z 368.1565 (1a). In the MS2 spectrum targeting the ion at m/z 420.1182 (Figure S5b), MS2 ions at m/z 340.1617 (2a), m/z 274.0856 (2b), and m/z 194.1290 (2c) were observed. These were most likely produced by the breakdown of the ion at m/z 420.1182 through processes such as sulfate elimination, uracil ring modification and opening of the tricyclic ring.

8. Positive mode Q-Exactive tandem mass spectra of ANA

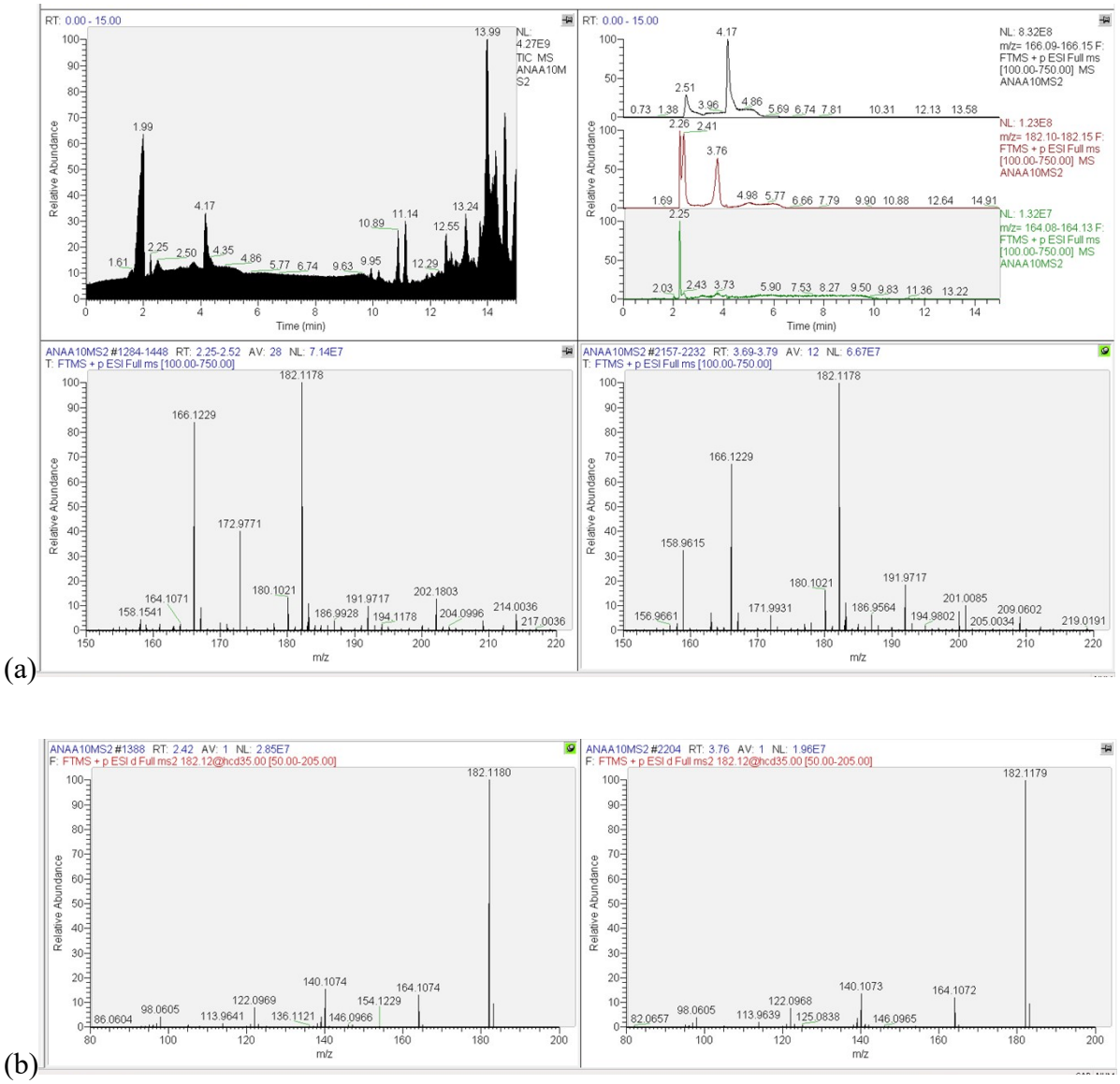

Figure S6: (a) Reaction product ion spectra MS^1 for ions eluting at 2.42 and 3.76 min and reconstructed ion chromatograms showing elution profiles of two ions (*m/z* 166 and 182); (b) CID product ion spectra MS^2 for ion *m/z* 182 eluting at 2.42 min and 3.76 min.

Two epoxy-ANA (m/z 182.1180 and m/z 182.1179) ions were observed with different retention times (Figure S6a). Each m/z 182 ion was selected in turn for MS2 fragmentation and each yielded the same legitimate product ions (Figure S6b), m/z 182.1180 > 164.1074, 146.0966, 140.1074, and 122.0969, m/z 182.1179 > 164.1072, 146.0965, 140.1073, and 122.0968, which are in accord with the results obtained in previous studies of the MS2 fragmentation products for the epoxy-ANA molecular ion ([M+H]+, m/z 182) (10, 11).

1. Isquith A, Abbott E, Walters P. Surface-bonded antimicrobial activity of an organosilicon quaternary ammonium chloride. Applied microbiology. 1972;24(6):859-63.
2. Walters P, Abbott E, Isquith A. Algicidal activity of a surface-bonded organosilicon quaternary ammonium chloride. Applied microbiology. 1973;25(2):253-6.
3. Nikawa H, Ishida K, Hamada T, Satoda T, Murayama T, Takemoto T, et al. Immobilization of octadecyl ammonium chloride on the surface of titanium and its effect on microbial colonization in vitro. Dental materials journal. 2005;24(4):570-82.
4. McMorn P, Hutchings GJ. Heterogeneous enantioselective catalysts: strategies for the immobilisation of homogeneous catalysts. Chemical Society Reviews. 2004;33(2):108-22.
5. Sakpal T, Kumar A, Kamble S, Kumar R. Carbon dioxide capture using amine functionalized silica gel. Indian Journal of Chemistry-Part A InorganicPhysical Theoretical and Analytical. 2012;51(9):1214.
6. Shimizu I, Yoshino A, Okabayashi H, Nishio E, J. O'Connor C. Kinetics of interaction of 3-aminopropyltriethoxysilane on a silica gel surface using elemental analysis and diffuse reflectance infrared Fourier transform spectra. Journal of the Chemical Society, Faraday Transactions. 1997;93(10):1971-9.
7. Metcalf J, Beattie K, Saker M, Codd G. Effects of organic solvents on the high performance liquid chromatographic analysis of the cyanobacterial toxin cylindrospermopsin and its recovery from environmental eutrophic waters by solid phase extraction. FEMS microbiology letters. 2002;216(2):159-64.
8. Foss AJ, Aubel MT. The extraction and analysis of cylindrospermopsin from human serum and urine. Toxicon. 2013;70:54-61.
9. Matilainen A, Gjessing ET, Lahtinen T, Hed L, Bhatnagar A, Sillanpää M. An overview of the methods used in the characterisation of natural organic matter (NOM) in relation to drinking water treatment. Chemosphere. 2011;83(11):1431-42.
10. James KJ, Crowley J, Hamilton B, Lehane M, Skulberg O, Furey A. Anatoxins and degradation products, determined using hybrid quadrupole time-of-flight and quadrupole ion-trap mass spectrometry: forensic investigations of cyanobacterial neurotoxin poisoning. Rapid Communications in Mass Spectrometry. 2005;19(9):1167-75.
11. Roy-Lachapelle A, Solliec M, Bouchard MF, Sauvé S. Detection of cyanotoxins in algae dietary supplements. Toxins. 2017;9(3):76.